The un-symmetric hybridization of graphene surface plasmons incorporating graphene sheets and nano-ribbons

Yu Sun, Zheng Zheng, Jiangtao Cheng, Jianwei Liu, Jiansheng Liu, and Shuna Li

Citation: Applied Physics Letters **103**, 241116 (2013); doi: 10.1063/1.4848100
View online: http://dx.doi.org/10.1063/1.4848100
View Table of Contents: http://scitation.aip.org/content/aip/journal/apl/103/24?ver=pdfcov
Published by the AIP Publishing

The un-symmetric hybridization of graphene surface plasmons incorporating graphene sheets and nano-ribbons

Yu Sun,[1] Zheng Zheng,[1,a)] Jiangtao Cheng,[2] Jianwei Liu,[1] Jiansheng Liu,[1] and Shuna Li[1,3]
[1]*School of Electronic and Information Engineering, Beihang University, Beijing 100191, China*
[2]*Department of Mechanical and Energy Engineering, University of North Texas, Denton, Texas 76207, USA*
[3]*National Key Laboratory of Electronic Measurement Technology, North University of China, Taiyuan 030051, China*

(Received 17 October 2013; accepted 28 November 2013; published online 13 December 2013)

Un-symmetric hybridization of graphene surface plasmons (GSPs) in waveguides incorporating graphene nano-ribbons and an underlying graphene sheet is theoretically studied. By tuning the chemical potential of the sheet, the characteristics of the hybrid modes can be shifted from sheet-like toward ribbon-like. The performance of hybrid modes reaches the maximum when phase match is satisfied. Superior to symmetric ribbon pairs, the favorable hybrid modes can be tuned at their best states, while the other modes are suppressed. The hybrid waveguide GSPs mode supported by this structure could extend the propagation distance by 46% over that of the modes for ribbon pairs. © *2013 AIP Publishing LLC*. [http://dx.doi.org/10.1063/1.4848100]

Plasmons, the collective oscillations of conduction electrons, are the pillar stones of applications ranging from photonic meta-materials, quantum optics, photovoltaics, photodetectors to optical bio-sensing.[1] The unique electronic properties of graphene,[2] a two dimensional (2D) layer of carbon atoms packed in hexagonal lattice,[3,4] make it a promising platform to build plasmonic devices and systems at terahertz frequencies.[5] The graphene surface plasmons (GSPs) predicted by Jablan *et al.*[6] have received experimental confirmation recently.[7] Compared to surface plasmon polaritons (SPPs) in noble metals at infrared frequencies, the GSPs manifest unique tunability using external gates,[8] presumably long plasmon lifetime,[9] and deep sub-wavelength confinement.[10]

The plasmonic hybridization in pairs of identical graphene sheets[11] and graphene nano-ribbons (GNRs)[12] enhances the modal properties and enlightens the design of ultra compact device. However, the pairs of graphene sheets cannot provide lateral field confinement due to their one dimension (1D) structure. The GNR pairs could offer 2D wave guiding, but such structures are challenging to fabricate and sensitive to alignment errors. What's more, both of structures need to be covered by the same material of substrates due to the symmetric nature of such hybridization. Another kind of hybridization between photonic mode and metal plasmonic mode has attracted much interest in near-infrared frequencies.[13,14] While comparing to a typical value of ~1.03 for SPPs on metals,[15] the effective index of GSPs is capable of reaching ~70 at THz frequencies.[8] So the hybridization with photonic mode is weak in graphene based structures due to the huge phase mismatch.

To circumvent the above problem and find an alternative approach to enable hybridization, we present an un-symmetric hybrid plasmonic waveguide that incorporating GNRs and an underlying graphene sheet. By tuning the chemical potential of the graphene sheet, the characteristics of the hybrid modes can be shifted from sheet-like toward ribbon-like. The performance of hybrid modes reaches its maximum near the corresponding critical points. Superior to symmetric hybrid ribbon pairs, the favorable hybrid modes can be selected by detuning other modes. Furthermore, the propagation distance of proposed hybrid modes is extended due to the relatively high chemical potential of graphene sheet. By replacing the lower ribbon in GNR pairs with sheet, the proposed structure becomes easy to fabricate and integrate. The concept of un-symmetric hybrid GSP waveguide sparks the expectations for large-scale production of high-performance graphene-based devices.

The proposed waveguide shown in Fig. 1 consists of an underlying graphene sheet separated from a GNR (width w) by a buffer layer (thickness t). The substrate and buffer layer are KCl ($n = 1.46$), with air ($n = 1$) covering the rest regions. More GNRs or GNR-based devices can be defined on the buffer layer for planar integration. The graphene sheet is uniformly biased and tuned by the Au gates. Graphene's complex conductivity is governed by the Kubo formula, which relates to the radian frequency ω, charged particle scattering rate Γ, temperature T, and chemical potential μ_c.[16] The value of $\Gamma = hq_eV_F/(2\mu E_F)$ is estimated from the measured impurity-limited DC graphene mobility[4] $\mu \approx 10\,000\ \mathrm{cm}^2/(\mathrm{V\,s})$

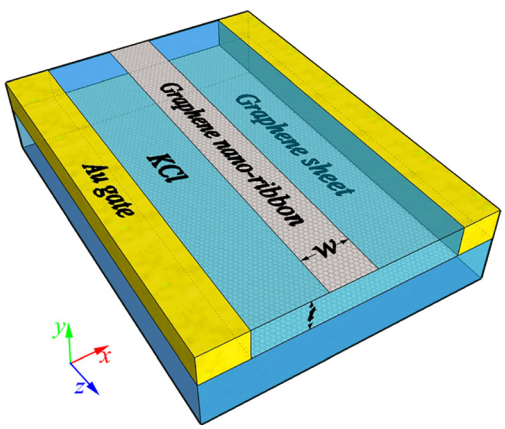

FIG. 1. Schematic of the proposed waveguide.

a)Email: zhengzheng@buaa.edu.cn

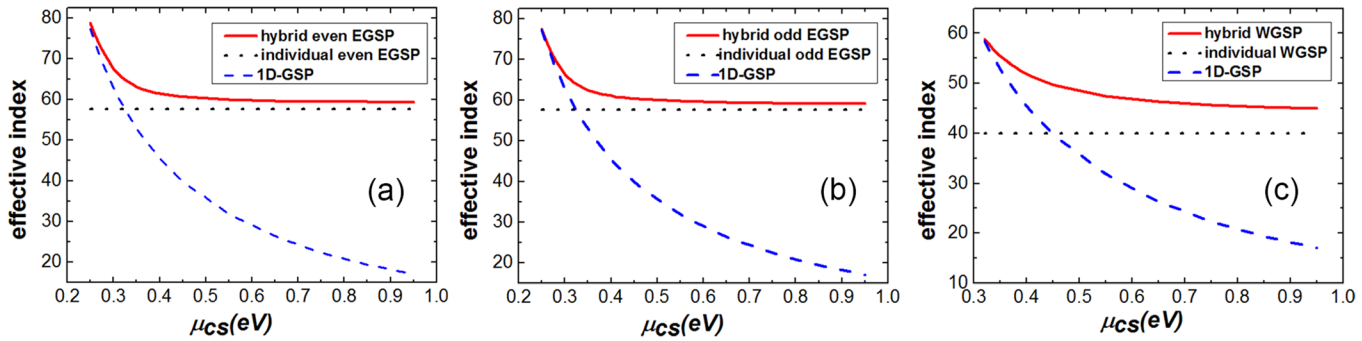

FIG. 2. Dependence of effective index on μ_{cs} for three hybrid modes.

for various Fermi levels E_F, where h is the Planck's constant, q_e is the charge of an electron, V_F is the Fermi velocity ($\sim 10^8$ cm/s in graphene).[17] To focus on the unique tunability of graphene, the geometric parameters w and t are fixed at 300 nm and 50 nm, respectively. The complex propagation constant β and field profiles are investigated at $\omega = 30$ THz, $T = 300$ K by the finite-element method (FEM) using COMSOL™. The eigenmode solver is used with the scattering boundary condition. Convergence tests are done to ensure that the numerical boundaries and meshing do not interfere with the solutions.

The chemical potential of GNR is doped at $\mu_{cr} = 0.3$ eV, while the chemical potential of sheet μ_{cs} can be tuned flexibly by external gate. The individual GNR (without the graphene sheet in Fig. 1) supports three modes:[18] the waveguide GSP (WGSP) mode with effective index $n_r = 40.0$, the even and odd hybridization of edge GSP (EGSP) modes with $n_r = 57.7$ and 57.5, respectively. The effective index n_h of the three hybrid GSP modes with different μ_{cs} is shown in Fig. 2. For illustration, the effective index of 1D-GSP modes supported by individual graphene sheet (without the GNR in Fig. 1) and corresponding GNR modes are also depicted. As shown in Fig. 2, all of the three GNR modes can hybrid with 1D-GSP modes and the hybrid modes evolve from sheet-like to ribbon-like asymptotically with increasing μ_{cs}. Different from the hybrid EGSP modes, the hybrid WGSP mode is cut off until μ_{cs} reaches 0.31 eV.

In order to gain a deeper understanding, the hybrid modes are analyzed using coupled-mode theory.[13] The hybrid modes are described as a superposition of the GNR waveguide and the graphene sheet waveguide modes: $n_h(\mu_{cs}) = an_r(\mu_{cr}) + bn_s(\mu_{cs})$, where a and b are the amplitude of constituent ribbon and sheet modes, respectively. The square norm of the ribbon mode amplitude $|a|^2$ is a measure of hybridization

$$|\mathrm{a}|^2 = \left.\frac{n_h(\mu_{cs}) - n_s(\mu_{cs})}{[n_h(\mu_{cs}) - n_r(\mu_{cr})] + [n_h(\mu_{cs}) - n_s(\mu_{cs})]}\right|_{\mu_{cr}=0.3\,\mathrm{eV}}. \quad (1)$$

In this respect, the mode is ribbon-like for $|a|^2 > 0.5$ and sheet-like otherwise. The dependence of $|a|^2$ on μ_{cs} is shown in Fig. 3. The profile of $|a|^2$ confirms the transition between ribbon-like and sheet-like modes. Fig. 4 depicts the electric field ($|E|$) profiles of hybrid modes with different μ_{cs}. As shown in Fig. 4, the concentrations of $|E|$ field shift from the underlying sheet toward the upper ribbon with increasing μ_{cs}. Fig. 3 also indicates the point of critical coupling: $\mu_{cs} = 0.45$ eV for the hybrid WGSP mode and 0.33 eV for both hybrid EGSP modes, respectively. The $|E|$ field profiles of critical coupling are shown in Figs. 4(b), 4(e) and 4(h). At the critical coupling points, the hybrid modes manifest equal ribbon and sheet characteristics ($|a|^2 = |b|^2 = 0.5$), corresponding to $n_r(\mu_{cr}) = n_s(\mu_{cs})$, indicating that two kinds of graphene plasma oscillations move in phase and maximize the effective optical capacitance of the waveguide.[13]

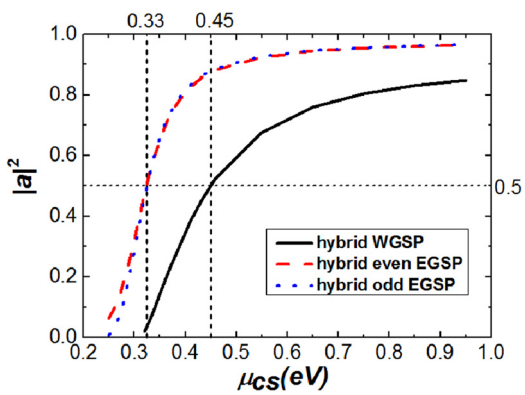

FIG. 3. Dependence of $|a|^2$ on μ_{cs} for three hybrid modes as modeled by the coupled mode theory.

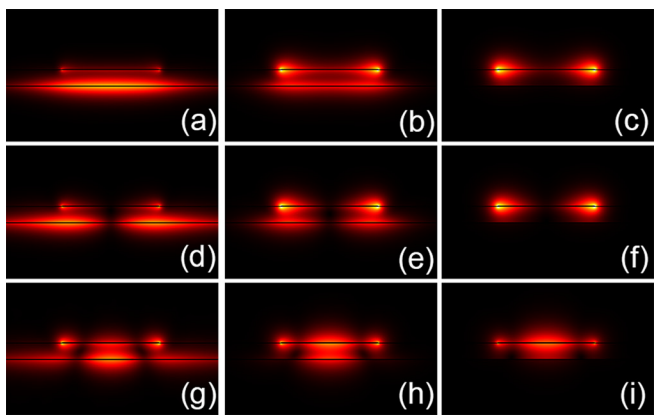

FIG. 4. $|E|$ profiles of hybrid even EGSP modes with (a) $\mu_{cs} = 0.25$ eV, (b) $\mu_{cs} = 0.33$ eV, (c) $\mu_{cs} = 0.95$ eV; $|E|$ profiles of hybrid odd EGSP modes with (d) $\mu_{cs} = 0.25$ eV, (e) $\mu_{cs} = 0.33$ eV, (f) $\mu_{cs} = 0.95$ eV; $|E|$ profiles of hybrid WGSP modes with (g) $\mu_{cs} = 0.32$ eV, (h) $\mu_{cs} = 0.45$ eV, (i) $\mu_{cs} = 0.95$ eV.

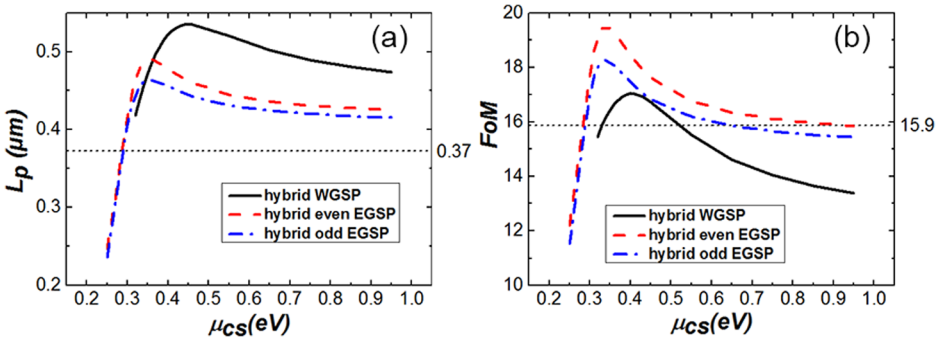

FIG. 5. Dependence of (a) propagation distance L_p and (b) figure of merit FoM on μ_{cs}. The short dotted lines indicate the L_p and FoM of symmetric hybrid WGSP mode in ribbon pairs.

The propagation length ($L_p = 2\pi/Im(\beta)$) and the figure of merit ($FoM = Re(\beta)/Im(\beta)$) that is also known as the propagation length expressed in terms of the plasmon wavelength ($\lambda_{spp} = \lambda_0/N_{eff}$)[19] of proposed structure are shown in Fig. 5. The propagation length of hybrid WGSP reaches the peak value (0.54 μm) at the critical coupling point. While the even and odd hybrid EGSP modes get the maximum (0.49 μm and 0.46 μm, respectively) slightly over the critical coupling point ($|a|^2 = 0.65$, $\mu_{cs} = 0.35$ eV). According to the Kubo formula, the higher chemical potential indicates a higher surface conductivity, which leads to a longer propagation distance of GSPs in the underlying graphene sheet.[19] In terms of propagation distance, slightly higher μ_{cs} is a good trade off between transmission loss and phase mismatch for tighter confined hybrid EGSP modes. So the GNR-based devices, e.g., graphene ring modulator,[20] can enhance their performance utilizing the proposed un-symmetric hybrid structure. Fig. 5(b) indicates that the FoM reaches the maximum near the critical coupling point and all the modes are capable of propagating more than 17 cycles. For comparison, the vertically offset ribbon pairs embedded in symmetric cladding KCl are simulated with the same parameters as the GNR in the proposed structure. In the hybrid modes of ribbon pairs, the even, hybrid WGSP mode performs best in terms of propagation length (0.37 μm) and FoM (15.9), which are indicated by short dotted lines in Figs. 5(a) and 5(b), respectively. Compared to the modes supported by the ribbon pairs, the increase in the propagation distance is at least 46%. Due to the differences in best performance points, the favorable hybrid modes can be tuned at their best states, while the other modes are suppressed.

In this paper, we put forward an un-symmetric hybrid plasmonic waveguide that incorporates GNRs in an underlying graphene sheet. The combination of the 1D sheet and 2D ribbon provides us an alternative avenue to further simplify the fabrication and improve modal characteristics. By optimizing the chemical potential of the underlying graphene sheet, the favorable hybrid modes can be tuned at their best states, while the other modes are suppressed. The concept of un-symmetric hybrid GSP waveguide indicates the strong potential for large-scale production of high-performance graphene-based devices.

This work was supported by 973 Program (2012CB315601) and NSFC (61107057/61221061).

[1]S. A. Maier, *Plasmonics: Fundamentals and Applications* (Springer, 2007).
[2]A. K. Geim and K. S. Novoselov, Nature Mater. **6**(3), 183 (2007); A. H. Castro Neto, F. Guinea, N. M. R. Peres, K. S. Novoselov, and A. K. Geim, Rev. Mod. Phys. **81**(1), 109 (2009).
[3]K. S. Novoselov, A. K. Geim, S. V. Morozov, D. Jiang, M. I. Katsnelson, I. V. Grigorieva, S. V. Dubonos, and A. A. Firsov, Nature **438**(7065), 197 (2005).
[4]K. S. Novoselov, A. K. Geim, S. V. Morozov, D. Jiang, Y. Zhang, S. V. Dubonos, I. V. Grigorieva, and A. A. Firsov, Science **306**(5696), 666 (2004).
[5]A. N. Grigorenko, M. Polini, and K. S. Novoselov, Nat. Photonics **6**(11), 749 (2012).
[6]M. Jablan, H. Buljan, and M. Soljačić, Phys. Rev. B **80**(24), 245435 (2009).
[7]L. Ju, B. Geng, J. Horng, C. Girit, M. Martin, Z. Hao, H. A. Bechtel, X. Liang, A. Zettl, Y. Ron Shen, and F. Wang, Nat. Nanotechnol. **6**(10), 630 (2011).
[8]P. A. Huidobro, M. L. Nesterov, L. Martín-Moreno, and F. J. García-Vidal, Nano Lett. **10**(6), 1985 (2010).
[9]H. Yan, Z. Li, X. Li, W. Zhu, P. Avouris, and F. Xia, Nano Lett. **12**(7), 3766 (2012); F. H. L. Koppens, D. E. Chang, and F. Javier García de Abajo, *ibid.* **11**(8), 3370 (2011).
[10]Z. Fei, A. S. Rodin, G. O. Andreev, W. Bao, A. S. McLeod, M. Wagner, L. M. Zhang, Z. Zhao, M. Thiemens, G. Dominguez, M. M. Fogler, A. H. Castro Neto, C. N. Lau, F. Keilmann, and D. N. Basov, Nature **487**(7405), 82 (2012); J. Chen, M. Badioli, P. Alonso-González, S. Thongrattanasiri, F. Huth, J. Osmond, M. Spasenović, A. Centeno, A. Pesquera, P. Godignon, A. Z. Elorza, N. Camara, F. J. Garcia de Abajo, R. Hillenbrand, and F. H. L. Koppens, Nature **487**(7405), 77 (2012).
[11]B. Wang, X. Zhang, X. Yuan, and J. Teng, Appl. Phys. Lett. **100**(13), 131111 (2012).
[12]J. Christensen, A. Manjavacas, S. Thongrattanasiri, F. H. L. Koppens, and F. Javier García de Abajo, ACS Nano **6**(1), 431 (2012).
[13]R. F. Oulton, V. J. Sorger, D. A. Genov, D. F. P. Pile, and X. Zhang, Nat. Photonics **2**(8), 496 (2008).
[14]Y. Bian, Z. Zheng, Y. Liu, J. Liu, J. Zhu, and T. Zhou, Opt. Express **19**(23), 22417 (2011).
[15]W. L. Barnes, A. Dereux, and T. W. Ebbesen, Nature **424**(6950), 824 (2003).
[16]L. A. Falkovsky and A. A. Varlamov, Eur. Phys. J. B **56**(4), 281 (2007).
[17]J. S. Gómez-Díaz, M. Esquius-Morote, and J. Perruisseau-Carrier, Opt. Express **21**(21), 24856 (2013).
[18]A. Yu Nikitin, F. Guinea, F. J. García-Vidal, and L. Martín-Moreno, Phys. Rev. B **84**(16), 161407 (2011).
[19]A. Vakil and N. Engheta, Science **332**(6035), 1291 (2011).
[20]M. Midrio, S. Boscolo, M. Moresco, M. Romagnoli, C. De Angelis, A. Locatelli, and A. D. Capobianco, Opt. Express **20**(21), 23144 (2012).